An improved potential energy curve for the ground state of NaK

J. Phys. B: At. Mol. Opt. Phys. **33** (2000) 2753–2762. Printed in the UK PII: S0953-4075(00)50114-X

An improved potential energy curve for the ground state of NaK

I Russier-Antoine, A J Ross, M Aubert-Frécon, F Martin and P Crozet

Laboratoire de Spectrométrie Ionique et Moléculaire (UMR 5579), Bâtiment 205, Université Lyon I et CNRS, Campus La Doua, 69622 Villeurbanne Cédex, France

Received 13 January 2000, in final form 17 April 2000

Abstract. This paper presents an accurate potential curve for the ground state of the NaK molecule. A series of resolved laser-induced fluorescence spectra of the A–X system allowed a spread of rotational levels in the lowest 70 vibrational levels (99.9% of the total well depth) to be observed. A variational method combining the inverted perturbation approach of Vidal and Scheingraber (Vidal C R and Scheingraber H 1977 *J. Mol. Spectrosc.* **65** 46) for short internuclear distances with an analytical expression for internuclear distances beyond 8.5 Å has been used to construct a potential energy curve which reproduces the measured ground state energies with an rms error of 0.003 cm^{-1}. The dissociation energy and coulombic parameters governing the Na(3s) + K(4s) interaction derived from this potential curve are compared with recent values.

1. Introduction

In view of the renewed interest in the long-range interactions between alkali atoms which has arisen with the developments of photoassociation techniques in ultracold alkali species, we undertook this work to give a reliable description of the electronic ground state of NaK. The ground state of NaK has been investigated before, both in resolved fluorescence experiments [1] and at high resolution in microwave spectroscopy [2,3]. In 1997, reduced potential calculations of Jenc [4] showed that the potential curve given by Ross *et al* in [1] was flawed, and in 1998, Krou-Adohi and Giraud-Cotton carefully reanalysed all the available data, and published an improved potential curve [5]. The reanalysis nevertheless suffered from the lack of observations in certain regions of the potential (the levels $47 \leqslant v \leqslant 56$ were not observed at all, and the measurements for $57 < v < 66$ were limited to a small selection of rotational levels). The interpolation over ten vibrational levels led to a more reasonable potential curve, but one which turns out not to match more recent measurements. This paper presents the potential curve for the ground state of NaK which has been constructed, having measured transitions involving many rovibrational levels up to $v = 70$ to supplement the existing database.

2. Experiment

We chose to use the strong $A\,^1\Sigma^+$–$X\,^1\Sigma^+$ system of NaK to study the ground state. Although the $A\,^1\Sigma^+$ state is inconvenient because of its strong interactions with the neighbouring $b\,^3\Pi$ state, it offers favourable Franck–Condon factors to most of the vibrational levels of the ground state (figure 1). NaK molecules were formed in a heatpipe containing a mixture of sodium and potassium metals, and 6 mbar of argon as a buffer gas. The heatpipe was operated at

0953-4075/00/142753+10$30.00

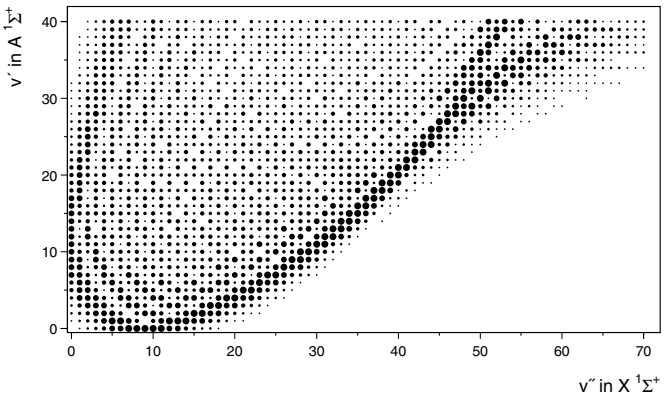

Figure 1. The Franck–Condon pattern for the A–X system of NaK.

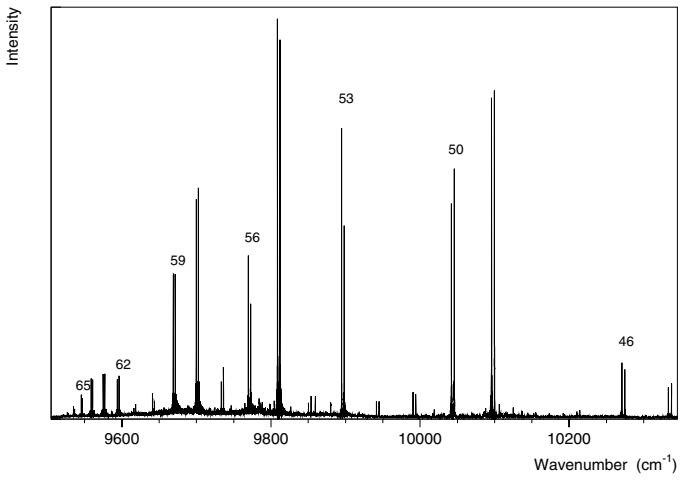

Figure 2. Part of a fluorescence spectrum, showing transitions to high levels of X (v'' levels are indicated). The laser (14 098.43 cm^{-1}) excited P(17) 35–5 in the A–X system. Resolution: 0.07 cm^{-1}, recording time about 30 min.

about 400 °C. A cw tuneable single-mode dye laser operating with LD 700 dye at typical powers of 250 mW, was used to excite selected levels of the A $^1\Sigma^+$ state which supplied a balanced spread of observations in v'' and J'' in the X $^1\Sigma^+$ state. Laser-induced fluorescence was recorded on a Fourier transform spectrometer at a resolution of 0.07 cm^{-1}, using a liquid-nitrogen-cooled InGaAs detector. Although the transitions close to the laser line were far from the peak response of the detector (1.3 μm), the entire A–X spectrum could be recorded without changing detectors, reducing the risk of calibration errors between different parts of the spectrum. Part of an A $^1\Sigma^+$–X $^1\Sigma^+$ fluorescence spectrum is illustrated in figure 2.

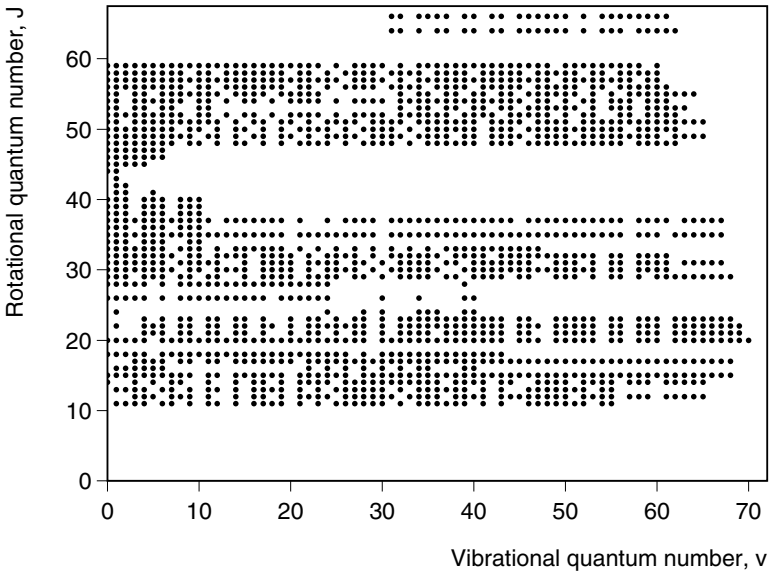

Figure 3. Range of rovibrational levels of the X state covered in the fit.

3. Data reduction

Molecular constants for the ground state of NaK were determined from a data set containing the 1736 newly measured A $^1\Sigma^+ - $ X $^1\Sigma^+$ lines, 411 B $^1\Pi$–X $^1\Sigma^+$ transitions recorded at a resolution of 0.03 cm^{-1} from [1], and 88 high-resolution rotation–vibration microwave transitions listed by Yamada and Hirota [3]. The data field is illustrated in figure 3. Data reduction was performed using a linear least-squares fitting routine. The ground state energies were represented by a Dunham-type expansion,

$$T''_{v,J} = \sum_{i,k} Y_{ik}(v + \tfrac{1}{2})^i [J(J+1)]^k. \tag{1}$$

The A $^1\Sigma^+$ state energies were treated as independent term energies, and the B $^1\Pi$ state energies by spectroscopic parameters:

$$T'_{v,J} = G_v + B_v[J(J+1) - 1] - D_v[J(J+1) - 1]^2 + \delta q_v[J(J+1)]$$

where $\delta = 0$ for levels of f parity and $\delta = 1$ for levels of e parity of B $^1\Pi$.

The fitting process was very straightforward for ground state levels up to $v = 62$, but parameter correlation became a problem when the higher levels were to be included in the fit. The distortion constants $D_{v''}$ and $H_{v''}$ become very large close to the dissociation limit, and the corresponding Dunham coefficients were not well determined from a direct fit to ground state energies. Reasonable guesses for the distortion constants $D_{v''}$, $H_{v''}$ and $L_{v''}$ were obtained by fitting the G_v and B_v constants up to $v = 62$ to a near-dissociation expansion using Le Roy's program VIBNDE, and using these parameters to calculate an RKR curve up to $v = 70$. Distortion terms were calculated from this curve using Le Roy's program LEVEL, and then fitted to a power series in $(v + \frac{1}{2})$. The least-squares fitting routine was then used to determine Y_{i0} and Y_{i1} terms only. By fixing the distortion parameters Y_{i2}, Y_{i3} and Y_{i4}, some

transitions to levels $63 \leqslant v \leqslant 67$ were gradually incorporated in the fit, but for the highest v, J levels observed, this was still unsatisfactory, and spectroscopic constants (G_v, B_v, D_v, H_v, ...) were finally used to represent term energies with $v \geqslant 62$. The complete set of energy levels for the ground state can be recalculated with the Dunham constants given in table 1 and the spectroscopic constants of table 2. No errors have been included in these tables because many more significant digits are required to reproduce the energies than could be statistically determined. The constants of table 2 are to be used with caution. Although they recalculate the observed levels very well (rms deviation 0.004 cm^{-1}), they are not likely to extrapolate very well to higher rotational levels. It is already clear in table 2 that the distortion constants increase very quickly with v, and the table truncates the series in $J(J+1)$ at the fifth-order term. Taking as an example the highest observed level in $v = 68$ ($J = 29$), the term $H_v[J(J+1)]^3$ contributes 0.119 cm^{-1} to the total energy, the term $L_v[J(J+1)]^4$ contributes 0.051 cm^{-1} and the term $M_v[J(J+1)]^5$ contributes 0.021 cm^{-1} so the next term in the series will become significant at higher J.

4. The potential curve

The Dunham coefficients listed in table 1 were used to generate an RKR curve, required as input for the inverted perturbation approach (IPA) program [6]. The IPA method was used to refine this curve by ensuring that the molecular energies calculated from the potential curve matched those given by the constants of table 1 (for $v \leqslant 61$) or those of table 2 (for $62 \leqslant v \leqslant 69$). The resulting IPA potential is presented in table 3. This curve differs significantly from the best available curve prior to our recent measurements, as shown in figure 4. It reproduces the measured term energies of bound rovibrational levels in the ground state with an rms error of 0.0032 cm^{-1}, a significant improvement on the earlier RKR curves given in [1, 4]. It did not perform so well for the quasibound levels lying above the adiabatic dissociation limit, suggesting that the uppermost part of the curve is not reliable. The outer turning point for $v = 69$ is at 11.5 Å, and it is possible to represent the outer part of the molecular potential by

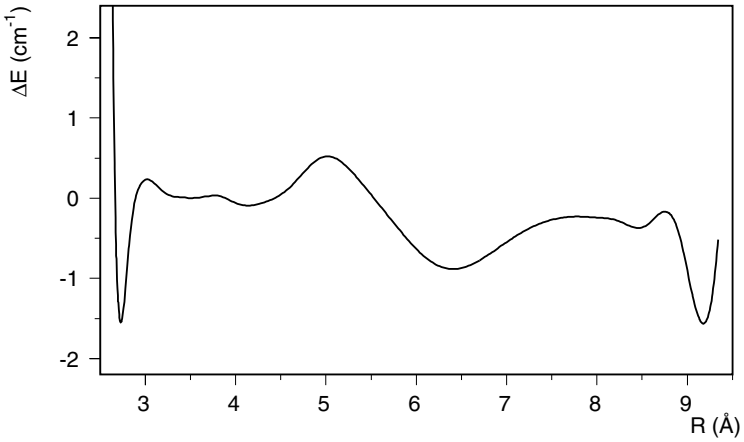

Figure 4. Difference in energy between the RKR potential of [5] and the potential given in table 5 as a function of R.

Table 1. Dunham-type coefficients for the ground state of NaK, valid for $v \leqslant 62$. Fluorescence transitions (1695 lines) in the A–X system were recalculated with an rms error of 0.003 cm^{-1}, the B–X transitions (411 lines) with an rms error of 0.004 cm^{-1} and the 88 microwave transitions with an rms error of 0.0002 cm^{-1}.

i	Y_{i0}	Y_{i1}	Y_{i2}	Y_{i3}	Y_{i4}
0	−0.024 2	$0.952\,290\,83 \times 10^{-1}$	$-0.225\,147\,47 \times 10^{-6}$	$0.523\,993\,00 \times 10^{-12}$	$-0.285\,307\,86 \times 10^{-17}$
1	124.008 69	$-0.446\,715\,11 \times 10^{-3}$	$-0.693\,798\,10 \times 10^{-9}$	$0.464\,012\,90 \times 10^{-15}$	$-0.234\,171\,69 \times 10^{-18}$
2	−0.485 187 40	$-0.401\,190\,66 \times 10^{-5}$	$-0.384\,508\,84 \times 10^{-9}$	$0.892\,976\,98 \times 10^{-15}$	$0.379\,657\,48 \times 10^{-19}$
3	$-0.321\,439\,96 \times 10^{-2}$	$0.367\,299\,87 \times 10^{-6}$	$0.670\,005\,14 \times 10^{-10}$	$-0.931\,093\,47 \times 10^{-16}$	$-0.396\,262\,21 \times 10^{-20}$
4	$0.312\,990\,10 \times 10^{-3}$	$-0.546\,477\,86 \times 10^{-7}$	$-0.648\,463\,59 \times 10^{-11}$	$0.284\,800\,50 \times 10^{-17}$	$0.166\,216\,17 \times 10^{-21}$
5	$-0.287\,230\,65 \times 10^{-4}$	$0.426\,995\,77 \times 10^{-8}$	$0.369\,114\,27 \times 10^{-12}$	$-0.267\,313\,00 \times 10^{-17}$	$-0.205\,778\,78 \times 10^{-23}$
6	$0.161\,262\,12 \times 10^{-5}$	$-0.210\,187\,54 \times 10^{-9}$	$-0.130\,878\,75 \times 10^{-13}$	$0.622\,875\,32 \times 10^{-18}$	$-0.929\,619\,44 \times 10^{-25}$
7	$-0.607\,924\,76 \times 10^{-7}$	$0.665\,461\,63 \times 10^{-11}$	$0.292\,288\,42 \times 10^{-15}$	$-0.620\,874\,07 \times 10^{-19}$	$0.361\,756\,86 \times 10^{-26}$
8	$0.154\,551\,35 \times 10^{-8}$	$-0.135\,777\,05 \times 10^{-12}$	$-0.401\,394\,65 \times 10^{-17}$	$0.342\,431\,39 \times 10^{-20}$	$0.204\,732\,10 \times 10^{-26}$
9	$-0.262\,022\,71 \times 10^{-10}$	$0.172\,451\,53 \times 10^{-14}$	$0.332\,303\,66 \times 10^{-19}$	$-0.115\,662\,10 \times 10^{-21}$	$-0.332\,086\,35 \times 10^{-27}$
10	$0.284\,011\,46 \times 10^{-12}$	$-0.124\,047\,85 \times 10^{-16}$	$-0.217\,070\,93 \times 10^{-21}$	$0.244\,686\,22 \times 10^{-23}$	$0.230\,165\,73 \times 10^{-28}$
11	$-0.178\,199\,48 \times 10^{-14}$	$0.385\,677\,32 \times 10^{-19}$	$0.196\,076\,47 \times 10^{-23}$	$-0.314\,428\,01 \times 10^{-25}$	$-0.462\,347\,71 \times 10^{-30}$
12	$0.493\,105\,77 \times 10^{-17}$		$-0.114\,135\,62 \times 10^{-25}$	$0.222\,869\,72 \times 10^{-27}$	$-0.162\,673\,67 \times 10^{-31}$
13				$-0.663\,676\,90 \times 10^{-30}$	$0.100\,224\,99 \times 10^{-32}$
14					$-0.205\,836\,09 \times 10^{-34}$
15					$0.196\,939\,09 \times 10^{-36}$
16					$-0.742\,126\,48 \times 10^{-39}$

Table 2. Parameters used to calculate energies of high-lying observed levels of the ground state (in cm^{-1}). Values marked with an asterisk were generated from the potential curve, and not determined in the fit. Only one level of $v = 70$ was observed, $T_{(v=70,J=20)} = 5274.548\ cm^{-1}$.

v	G_v	$100\ B_v$	$10^6\ D_v$	$10^{10}\ H_v$	$10^{13}\ L_v$	$10^{16}\ M_v$
62	5184.5461	3.408 61	1.220 37	0.572 79	−0.002 083	
63	5204.4412	3.141 08	1.161 75	−0.398 78	−0.001 78	−0.025 862
64	5221.4349	2.859 86	0.095 23	−4.779 97	1.955 4	−0.371 031
65	5235.5764	2.589 06	1.218 28	−4.161 26	2.203 8	−0.591 249
66	5246.9685	2.332 08	2.158 05	4.136 23	−1.937 4	−0.056 6*
67	5255.8027	2.101 46	3.995 31	20.811 6	−8.463 9	−0.131 9*
68	5262.4929	1.749 21	2.372 51	−1.808 38	−0.896*	−0.427 8*
69	5267.2863	1.420 42	2.333*	−4.416*	−2.172*	−1.466*

asymptotic formulae at such a distance. The outer part of the rotationless IPA curve ($R > 8.5$ Å) was therefore replaced by an analytical extension of the form

$$V(R) = D_e - \sum_{n=6,8,10} \chi_n(R) \cdot \frac{C_n}{R^n} - E_{\text{exchange}}(R). \tag{2}$$

The damping function χ_n was established from the IPA curves of the X $^1\Sigma^+$ state (table 3) and the a $^3\Sigma^+$ state (published in [7]): using a cubic spline function to interpolate between the points available, an average curve was generated as a function of R. In a crude picture, in which overlap between the Na and K orbitals is assumed to be small, the average curve $\frac{1}{2}(E_{X\,^1\Sigma^+}(R) + E_{a\,^3\Sigma^+}(R))$ is unaffected by exchange contributions, and can be expressed simply as an attenuated multipolar expansion:

$$E_{\text{average}} = D_e - \sum_{n=6,8,10} \chi_n(R) \cdot \frac{C_n}{R^n} \tag{3}$$

The damping function $\chi_n(R)$ is introduced to take into account the effect of overlap on the coulombic interaction energy. We took a functional form very close to that proposed by Varandas and Voronin [8],

$$\chi_n(R) = \left\{1 - \exp\left[-\frac{A_n R}{\rho} - \frac{B_n R^2}{\rho^2}\right]\right\}^n$$

with $\rho = 29.5994\ a_0$ (following [8]), $\rho = 5.5 + 1.25(\sqrt{\langle r^2\rangle_{Na(3s)}} + \sqrt{\langle r^2\rangle_{K(4s)}})\ a_0$, $A_n = \gamma n^{-0.701\,72}$ (γ is a variable parameter here, as opposed to 16.66 in [8]), $B_n = 17.193\,38 \exp(-0.095\,74n)$.

The ground state exchange energy was simply parametrized by

$$E_{\text{exchange}}(R) = A \exp(-\alpha R - \beta R^2). \tag{4}$$

This unusual form was adopted after having calculated the exchange energy using formulae given by Hadinger *et al* [9] for the ground state of a heteronuclear alkali diatomic, based on the formalism developed by Smirnov and Chibisov [10]. We found that the exchange energy as defined by

$$2E_{\text{exchange}}(R) = E_{a\,^3\Sigma^+}(R) - E_{X\,^1\Sigma^+}(R) \tag{5}$$

could be satisfactorily reproduced by the formulae given in [9] (errors of the order of 1 cm^{-1} at 8 Å using theoretically determined parameters, and of 0.02 cm^{-1} at 8 Å if the atomic parameters were optimized), but that when this exchange energy is taken in equation (2) for the ground state, the coulombic parameters could not generate a sufficiently accurate molecular potential to reproduce the observed energies. We therefore used equations (2) and (4) to represent the ground state potential of table 3, considering A, α and β as fitting parameters only. They

Table 3. Turning points generated by IPA.

v	G_v (cm^{-1})	$R_{\min}$(Å)	$R_{\max}$(Å)	v	G_v (cm^{-1})	$R_{\min}$(Å)	$R_{\max}$(Å)
−1/2	−0.0245	3.499 04					
0	61.8578	3.367 16	3.641 80	36	3787.1313	2.648 13	5.429 38
1	184.8878	3.276 79	3.754 15	37	3866.2152	2.640 90	5.480 86
2	306.9250	3.217 42	3.835 79	38	3943.6579	2.633 93	5.533 58
3	427.9596	3.170 77	3.904 97	39	4019.4214	2.627 20	5.587 67
4	547.9837	3.131 57	3.966 99	40	4093.4662	2.620 70	5.643 25
5	666.9900	3.097 39	4.024 26	41	4165.7510	2.614 44	5.700 47
6	784.9715	3.066 90	4.078 14	42	4236.2323	2.608 40	5.759 48
7	901.9206	3.039 26	4.129 48	43	4304.8650	2.602 56	5.820 46
8	1017.8293	3.013 91	4.178 84	44	4371.6021	2.596 93	5.883 61
9	1132.6889	2.990 46	4.226 64	45	4436.3944	2.591 50	5.949 14
10	1246.4898	2.968 61	4.273 18	46	4499.1911	2.586 26	6.017 32
11	1359.2220	2.948 14	4.318 72	47	4559.9391	2.581 23	6.088 41
12	1470.8747	2.928 87	4.363 43	48	4618.5838	2.576 41	6.162 76
13	1581.4368	2.910 65	4.407 48	49	4675.0682	2.571 80	6.240 73
14	1690.8964	2.893 38	4.451 00	50	4729.3337	2.567 43	6.322 76
15	1799.2410	2.876 95	4.494 10	51	4781.3198	2.563 29	6.409 35
16	1906.4577	2.861 29	4.536 87	52	4830.9640	2.559 41	6.501 09
17	2012.5328	2.846 33	4.579 41	53	4878.2024	2.555 78	6.598 69
18	2117.4521	2.832 01	4.621 79	54	4922.9698	2.552 41	6.703 00
19	2221.2007	2.818 29	4.664 08	55	4965.2001	2.549 28	6.815 02
20	2323.7628	2.805 11	4.706 35	56	5004.8270	2.546 41	6.936 00
21	2425.1221	2.792 45	4.748 67	57	5041.7850	2.543 77	7.067 47
22	2525.2614	2.780 26	4.791 09	58	5076.0107	2.541 37	7.211 31
23	2624.1624	2.768 53	4.833 67	59	5107.4453	2.539 19	7.369 95
24	2721.8063	2.757 22	4.876 48	60	5136.0363	2.537 23	7.546 45
25	2818.1730	2.746 31	4.919 56	61	5161.7420	2.535 46	7.744 84
26	2913.2415	2.735 78	4.962 98	62	5184.5357	2.533 90	7.970 43
27	3006.9899	2.725 62	5.006 79	63	5204.4120	2.532 53	8.230 41
28	3099.3951	2.715 80	5.051 05	64	5221.3948	2.531 35	8.534 72
29	3190.4328	2.706 31	5.095 83	65	5235.5475	2.530 36	8.897 36
30	3280.0778	2.697 13	5.141 18	66	5246.9860	2.529 55	9.338 44
31	3368.3035	2.688 26	5.187 18	67	5255.8912	2.528 92	9.887 27
32	3455.0824	2.679 68	5.233 88	68	5262.5206	2.528 44	10.586 61
33	3540.3856	2.671 39	5.281 37	69	5267.2077	2.528 11	11.498 63
34	3624.1827	2.663 37	5.329 73	70	5272.2876	2.527 75	14.412 11
35	3706.4423	2.655 62	5.379 03				

overestimate the 'exchange' contribution as defined by equation (5), but recalculate the IPA potential from 7 to 11.5 Å. The long-range parameters (equations (2) and (4)) obtained from the IPA curve are given in table 4. A second set of long-range parameters was obtained by fitting not only the last nine points of the IPA curve (8–11.5 Å), but also 188 measured term energies for observed rotational levels with $63 \leqslant v \leqslant 70$. The measured energies were compared with those obtained by solving the radial Schrödinger equation using a numerical curve which was simply the IPA curve for $1.6 \leqslant R \leqslant 8.5$ Å, and whose outer part was optimized iteratively using new long-range parameters. These parameters are also listed in table 4, together with values found independently from the experimental work of Ishikawa *et al* [7] on the a $^3\Sigma^+$ state of NaK, and theoretical values for the leading terms in the multipolar expansion, C_6 and C_8 given by Marinescu and Sadeghpour [11].

Table 4. Parameters used to extrapolate the outer part of the potential curve of the $X\,^1\Sigma^+$ state, and comparison with coulombic parameters found in the literature. Uncertainties (1 standard deviation) are quoted in parentheses, in units of the last digit[a].

Parameter	Curve only	Curve + T_{vJ}	Theory [11]	a $^3\Sigma^+$ [7]	Hybrid X, a [12]
D_e (cm^{-1})	5273.70 (3)	5273.696 (45)		5273.716 (19)	5273.65 (10)
$\gamma(a_0)$	13.0	13.02 (12)			
$10^{-7}C_6$ (cm^{-1} Å^6)	1.2154 (35)	1.2144 (46)	1.1566	1.275 (15)	1.1316
$10^{-8}C_8$ (cm^{-1} Å^8)	2.9619[b]	2.9619[b]	2.9619	2.22 (19)	3.5278
$10^{-9}C_{10}$ (cm^{-1} Å^{10})	9.400[b]	9.400[b]	9.400	11.00 (61)	9.400
$10^{-5}A$ (cm^{-1})	6.578 (122)	6.578			
$10^{-4}\alpha$ (Å^{-1})	5.748 (18)	5.748			
β (Å^{-2})	737.5	737.5			
Number of data	18	197			
Rms error (cm^{-1})	0.005	0.006			

[a] Values in [11] were converted to C_n in cm^{-1} Å^n, by multiplying by $219\,474.632 \times (0.529\,1772)^n$. γ is used in the calculation of damping functions $\chi_n(R)$ (equation (3)). It was determined iteratively using the curve alone, but obtained simultaneously with C_6 and D_e in the fit of curve + energies. The exchange parameter β was determined iteratively using the curve alone.

[b] Constrained at theoretical values from [11].

The full potential curve is given in table 5. It can be used to calculate the observed energy levels with an rms error of 0.003 cm^{-1}. The largest errors were still associated with some (but not all) of the highest quasibound levels, the differences reaching $-0.026\,cm^{-1}$ for $T_{(v=61,J=64)} = 5293.437$ and $-0.030\,cm^{-1}$ for $T_{(v=64,J=55)} = 5294.253\,cm^{-1}$. The differences were less than $0.016\,cm^{-1}$ for the remaining quasibound levels, and never exceeded $0.012\,cm^{-1}$ for the observed bound levels. The errors were not really systematic, but possibly arise from difficulties in defining a reliable potential curve from very few observations in the high-energy region. We nevertheless feel that the curve should provide a good prediction of the highest $T_{v,J}$ levels ($v > 69$) of the ground state, where spectroscopic constants are not well defined.

5. Dissociation energy and long-range parameters

Because the long-range parameters given in table 4 were obtained by extrapolation of a potential curve which scarcely extends into the region of internuclear distances traditionally considered appropriate for the multipolar expansions of the type $V(R) = D_e - \sum \frac{C_n}{R^n}$, we were not entirely satisfied with the statistical errors associated with these values. Le Roy has shown [13] that near-dissociation expansion fits of vibrational energies can yield the dissociation energy, D_e, and the (non-integer) vibrational quantum number at dissociation v_D. The vibrational energies (generated from the potential curve in table 5) were therefore expressed as

$$G_v = D_e - X_0(n = 6, C_6, \mu)(v_D - v)^3 \left[\frac{L}{M}\right]^S \tag{6}$$

where $\frac{L}{M} = \frac{1+p_1(v_D-v)+p_2(v_D-v)^2+\cdots}{1+q_1(v_D-v)+q_2(v_D-v)^2+\cdots}$, and the power S is either 1 (so-called 'outer' expansion) or 3 ('inner' expansion). These near-dissociation expansions (unlike the Dunham polynomials) are designed to extrapolate correctly to the dissociation energy. Using Le Roy's routine VIBNDE, a selection of combinations of $[\frac{L}{M}]$ were tested, using nine or ten terms in the developments, taking $C_6 = 1.2144 \times 10^7$ cm^{-1} Å^6 and $C_8 = 2.9619 \times 10^9$ cm^{-1} Å^8 (table 4). The best NDE fits were those with almost equal numbers of terms in the numerator and denominator expansions. Inner and outer expansions worked equally well. Averaging over all the converging

Table 5. NaK X state potential curve, IPA curve plus extrapolation beyond 8.5 Å according to equation (2). Used with cubic spline interpolation and intervals of 0.0064 Å, this reproduces the full set of ground state energies (figure 3) with an rms error of 0.003 cm^{-1}.

R (Å)	V (cm^{-1})	R (Å)	V (cm^{-1})	R (Å)	V (cm^{-1})
2.20	11594.8205	3.41	27.5151	4.90	2774.6669
2.30	9104.0944	3.42	21.5596	5.00	2992.6125
2.40	7148.9304	3.43	16.3573	5.10	3198.7896
2.50	5641.1076	3.44	11.8954	5.20	3392.4155
2.52	5379.0866	3.45	8.1616	5.30	3573.0292
2.54	5095.6036	3.46	5.1439	5.40	3740.4516
2.56	4823.1326	3.47	2.8304	5.50	3894.7449
2.58	4574.8666	3.48	1.2098	5.60	4036.1749
2.60	4335.2158	3.49	0.2707	5.70	4165.1739
2.62	4101.5627	3.499	0.0028	5.80	4282.3053
2.64	3876.1750	3.50	0.0022	5.90	4388.2299
2.66	3659.7766	3.51	0.3935	6.00	4483.6737
2.68	3451.8645	3.52	1.4324	6.20	4646.1811
2.70	3251.9080	3.53	3.1073	6.40	4775.9576
2.72	3059.6364	3.54	5.4066	6.60	4878.7989
2.74	2874.9030	3.55	8.3190	6.80	4959.8628
2.76	2697.5617	3.56	11.8334	7.00	5023.5554
2.78	2527.4376	3.57	15.9392	7.20	5073.5304
2.80	2364.3427	3.58	20.6257	7.40	5112.7514
2.82	2208.0948	3.59	25.8827	7.60	5143.5817
2.84	2058.5259	3.60	31.7002	7.80	5167.8821
2.86	1915.4819	3.62	44.9761	8.00	5187.1056
2.88	1778.8181	3.64	60.3701	8.20	5202.3822
2.90	1648.3948	3.66	77.8011	8.40	5214.5790
2.92	1524.0743	3.68	97.1892	8.60	5224.3635
2.94	1405.7194	3.70	118.4575	8.80	5232.2613
2.96	1293.1930	3.72	141.5314	9.00	5238.6730
2.98	1186.3584	3.74	166.3370	9.20	5243.9111
3.00	1085.0800	3.76	192.8016	9.40	5248.2177
3.02	989.2236	3.78	220.8548	9.60	5251.7814
3.04	898.6573	3.80	250.4275	9.80	5254.7491
3.06	813.2510	3.82	281.4525	10.00	5257.2360
3.08	732.8771	3.84	313.8640	10.20	5259.3323
3.10	657.4104	3.86	347.5980	10.40	5261.1096
3.12	586.7276	3.88	382.5918	10.60	5262.6249
3.14	520.7076	3.90	418.7845	10.80	5263.9233
3.16	459.2310	3.92	456.1167	11.00	5265.0412
3.18	402.1798	3.94	494.5303	11.20	5266.0079
3.20	349.4376	3.96	533.9688	11.40	5266.8473
3.22	300.8889	3.98	574.3769	11.60	5267.5790
3.24	256.4198	4.00	615.7010	11.80	5268.2191
3.26	215.9173	4.10	834.2691	12.00	5268.7809
3.28	179.2693	4.20	1068.3980	13.00	5270.7459
3.30	146.3655	4.30	1312.7365	14.00	5271.8470
3.32	117.0967	4.40	1562.6259	15.00	5272.4949
3.34	91.3555	4.50	1814.0573	16.00	5272.8916
3.36	69.0340	4.60	2063.6173	17.00	5273.1427
3.38	50.0283	4.70	2308.4280	18.00	5273.3063
3.40	34.2368	4.80	2546.0945		

fits with nine and ten parameters, the NDE method gives

$$D_e = 5273.78 \pm 0.24 \text{ cm}^{-1}.$$

$$\upsilon_D = 74.3 \pm 0.3.$$

The average rms error was 0.005 cm^{-1} for the nine-parameter NDE fits and 0.003 cm^{-1} for the ten-parameter fits.

The value of D_e confirms the value 5273.70(4) cm^{-1} obtained by extrapolating the potential curve using asymptotic formulae for the coulombic and exchange energies. The NDE approach suggests that the error on the dissociation energy obtained from the potential curve is too small. The fits to the potential curve and the NDE fits both place D_e very close to the value of $5273.716 \pm 0.019 \text{ cm}^{-1}$ obtained from results published in a completely independent study of the a $^3\Sigma^+$ state of NaK by Ishikawa and co-authors [7]: $T_e(\text{a } ^3\Sigma^+) = 5065.858$ and $D_e(\text{a } ^3\Sigma^+) = 207.858(19) \text{ cm}^{-1}$. Both these experimental values are higher than the value 5273.65(10) cm^{-1} proposed very recently by Zemke and Stwalley [12], following a combined treatment of the IPA curve of [7] for the a $^3\Sigma^+$ state and a corrected ground state potential curve deduced from data in [1]. Our experimental value for the leading term C_6 $(1.214(5) \times 10^7 \text{ cm}^{-1} \text{ Å}^6)$ representing dispersion interactions between Na(3s) and K(4s) is larger than the theoretical prediction $(1.1665 \times 10^7 \text{ cm}^{-1} \text{ Å}^6)$, and smaller than the experimental value of $1.275(15) \times 10^7 \text{ cm}^{-1} \text{ Å}^6$ found from the a $^3\Sigma^+$ state [7]. Zemke and Stwalley [12] find a C_6 value which is closer to the theoretical value, but which does not give an equally satisfactory extrapolation of the IPA curve in table 3.

The discrepancies found in the C_6 coefficients arise when trying to separate the exchange and coulombic contributions to the molecular potential as overlap effects become significant. Since the asymptotic models for the exchange energy are designed to calculate the quantity $2E_{\text{exchange}}(R) = E_{\text{a } ^3\Sigma^+}(R) - E_{\text{X } ^1\Sigma^+}(R)$ (equation (5)), and the C_n coefficients depend only on atomic properties, the C_n must be common to both the singlet and triplet ground states. This work therefore indicates that the damping coefficients χ_n used in equation (3) need to vary not only as a function of R, but also according to electronic state. With insufficient observations at long internuclear distances to allow the 'true' C_n coefficients to be determined, we were unable to pursue this further at this stage, but it seems that equation (3) oversimplifies the situation, even for the interaction between two ground state alkali atoms.

Acknowledgment

We thank Professor R Le Roy, University of Waterloo, Canada, for making available the programs VIBNDE (copyright 1996) and LEVEL 6.1b (copyright 1998) used in this work.

References

[1] Ross A J, Effantin C, D'Incan J and Barrow R F 1985 *Mol. Phys.* **56** 903–12
[2] Wormsbecher R F, Hessel M M and Lovas F J 1981 *J. Chem. Phys.* **74** 6983–5
[3] Yamada C and Hirota E 1992 *J. Mol. Spectrosc.* **153** 91–5
[4] Jenc F 1997 Private communication
[5] Krou-Adohi A and Giraud-Cotton S 1998 *J. Mol. Spectrosc.* **190** 171–88
[6] Vidal C R and Scheingraber H 1977 *J. Mol. Spectrosc.* **65** 46–64
[7] Ishikawa K, Mukai N and Tanimura M 1994 *J. Chem. Phys.* **101** 876–81
[8] Varandas A J C and Voronin A I 1995 *Mol. Phys.* **85** 497–526
[9] Hadinger G, Hadinger G, Magnier S and Aubert-Frécon M 1996 *J. Mol. Spectrosc.* **175** 441–4
[10] Smirnov B M and Chibisov M I 1965 *Sov. Phys.–JETP* **21** 624–8
[11] Marinescu M and Sadeghpour H R 1999 *Phys. Rev.* A **59** 390–404
[12] Zemke W and Stwalley W C 1999 *J. Chem. Phys.* **111** 4956–61
[13] Le Roy R J 1980 *J. Chem. Phys.* **73** 6003–12
Le Roy R J 1994 *J. Chem. Phys.* **101** 10 217–28